Measuring Elastic Scattering in the Coulomb Nuclear Interference (CNI) Region in ATLAS - Total Cross Sections and Luminosity

M. Heller

Measuring Elastic Scattering in the Coulomb Nuclear Interference (CNI) Region in ATLAS – Total Cross Sections and Luminosity

Matthieu Heller, on behalf of the ATLAS collaboration

LAL, Orsay, Univ Paris-Sud, CNRS/IN2P3

DOI: will be assigned

ATLAS is being complemented with detectors to measure elastic scattering at small angles. This will give a possibility both to measure the total cross section and make an absolute luminosity calibration of the Luminosity monitors of ATLAS. The principle of the measurement, the experimental requirements and the detector performances found in a 2008 test-beam are presented in this article.

1 Introduction

The Large Hadron Collider (LHC) will provide proton-proton collisions for the experiments installed at the interaction points (IP). The ATLAS detector is designed to detect high p_t reactions and will focus on the discovery of the Higgs boson and new physics. However ATLAS is now also complemented by detectors in the very forward region to measure small angle elastic scattering. This will give a possibility to measure the total cross section and provide accurate luminosity calibration. The ultimate goal is to reach the Coulomb Nuclear Interference (CNI) region but even without reaching the CNI region precise luminosity calibration can be done. The detectors will be installed in so called "Roman Pots" 240 metres away from the ATLAS interaction point. The scattered particles at the IP will travel along the accelerator lattice and be detected by fiber trackers that are inserted in the Roman Pots. This measurement requires a special optics with very high beta at the interaction point and consequently will be done during dedicated runs.

2 Principle of the Measurement

The rate of elastic scattering is linked to the total interaction rate through the optical theorem, which states that the total cross section is directly proportional to the imaginary part of the nuclear forward elastic scattering amplitude extrapolated to zero momentum transfer:

$$\sigma_{tot} \propto \Im\left[F_n(t=0)\right]$$

At very small scattering angle the four-momentum transfer can be written $-t \approx (p\theta)^2$ where p refers to the beam momentum and θ to the scattering angle at the IP.

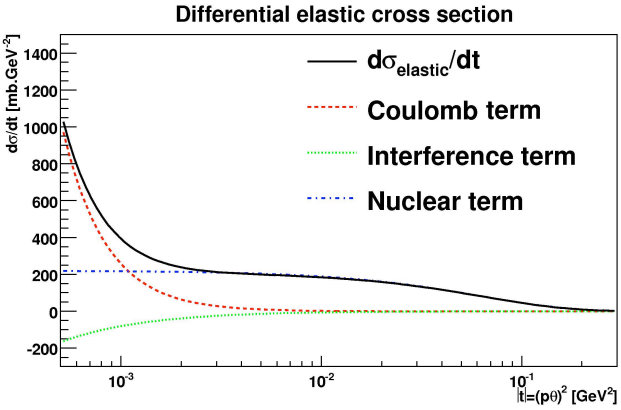

Figure 1: Contribution to the differential elastic cross section of the three components at small t value with σ_{tot}=100 mb, ρ=0.013 and b=18 GeV^{-2}.

Taking into account the optical theorem and the Coulomb term, the rate of elastic scattering at small t-values can be written as [1]:

$$\frac{dN}{dt} = L\pi \left| f_C + f_N \right|^2 \approx L\pi \left| \frac{-2\alpha}{|t|} + \frac{\sigma_{tot}}{4\pi} (i+\rho)\, e^{-b|t|/2} \right|^2 \tag{1}$$

where the first term corresponds to the Coulomb and the second to the strong interaction amplitude and α is the fine structure constant, σ_{tot} the total proton-proton cross section, b the nuclear slope and ρ the ratio of the real over the imaginary part of the forward elastic scattering amplitude. The formula is oversimplified, and there are also other corrections as the proton electromagnetic form factor and the relative phase between the Coulomb and the strong amplitude that are included in the final analysis. This expression allows to make the distinction between three terms as seen in Fig. 1. Fitting the rate of elastic scattering as a function of t allows to determine L, σ_{tot}, b and ρ.

3 Experimental Framework

The best absolute accuracy on the luminosity measurement is obtained by approaching as close as possible the Coulomb region where the correlation between the luminosity and the total cross section gets smaller. However at the TeV scale, this means measuring scattering angles of a couple of micro-radians.

At the nominal energy of the LHC (7 TeV) the strong amplitude is equal to the electromagnetic amplitude for $-t = 6\ 10^{-4}$ GeV^2. This corresponds to a scattering angle of 3.5 μrad. A direct measurement of this angle would require to intercept these protons before the first magnetic element. This is in practice impossible because the separation between these protons and the beam core is less than 200 μm. It was found that the best solution was to use dedicated optics which will separate enough the beam core and the elastically scattered protons at 240 m from the IP (see Fig. 2). In this location Roman Pots (RPs) detectors will be inserted to tag the elastic protons.

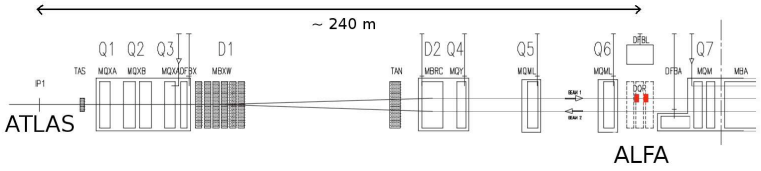

Figure 2: Location of the two stations (in red) on beam 1. Both other stations are on beam 2, on the opposite side with respect to ATLAS.

The beam conditions required to reach the CNI region are a small emittance and special beam optics. This dedicated beam optics is characterized by a very large β^* at the ATLAS IP, zero dispersion and a phase advance of the betatron function between the IP and the detectors of 90 degrees in the vertical plane to perform the parallel-to-point focussing which is sketched in Fig. 3. This has the consequence that particles scattered with the same angle arrive at the same position in the detector. An optics solution fulfilling the above requirements must be used in combination with rather few bunches of low intensity compared to nominal LHC settings. It will produce instantaneous luminosities in the range of 10^{27} to 10^{28} cm^{-2}s^{-1}.

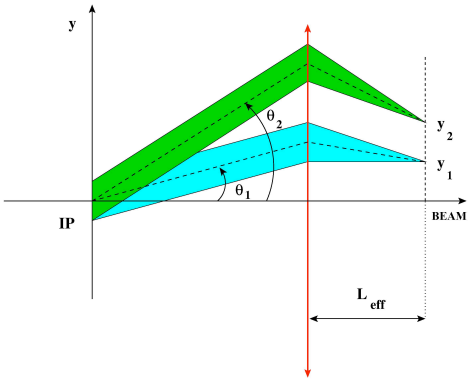

Figure 3: Parallel-to-point focussing where the optics brings all particles scattered with the same angle at the IP to the same location in the detector.

Using the expression of the scattering angle as a function of the position in the detector, the minimum t-value that we will be able to detect depends on the particle's momemtum (p), the distance to the beam centre expressed in terms of number of σ of the beam size (n_{min}), the emittance (ϵ), and the value of the betatron function at the IP (β_{IP}):

$$-t_{min} = p^2 n_{min}^2 \frac{\epsilon}{\beta_{IP}} \tag{2}$$

Assuming that we can approach the beam down to $12\,\sigma$, that we run at 7 TeV and that the normalised emittance is $\epsilon_N = 1\mu$m rad with a $\beta_{IP} = 2625$ m, we obtain $-t_{min} = 3.7\ 10^{-4}$ GeV^2 which is equivalent to $\theta_{IP,y} = 3\,\mu$rad.

To intercept these protons, two Roman Pot stations are installed symmetrically in the forward direction on beam 1 and beam 2. Each station is made of an upper and a lower

detector. The detectors inserted into the Roman Pots (RPs) are presented in the following section.

4 ALFA Detector

The ALFA detector[1] is made of a scintillating fiber tracker inserted in a Roman Pot (see Fig. 4). The tracker is made of 20 layers of 64 squared fibers each organised in a U-V geometry with 90° between two consecutive layers (see Fig. 5).

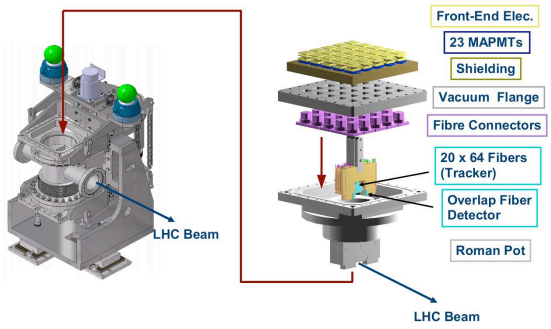

Figure 4: Schematic view of the ALFA detector.

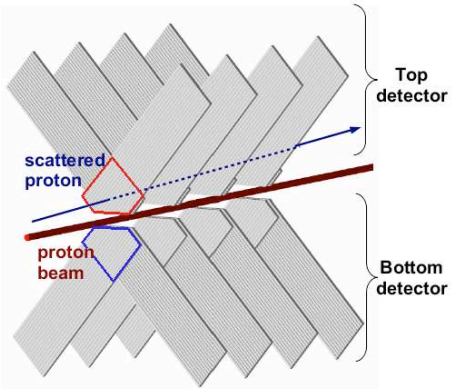

Figure 5: Schematic view of the main tracker. Only four U-V planes out of ten are represented on the picture.

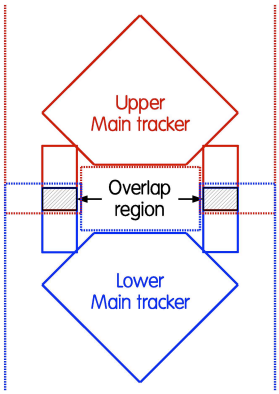

Figure 6: Schematic view of the overlap detectors.

The scintillating fibers are 0.5×0.5 mm^2 and a staggering of 10 % is applied between two consecutive planes providing a theoretical resolution close to 15 μm. However as shown in Section 6, the assembling imperfections worsen this result. Each layer is read out by a Multi Anode PhotoMulTiplier (MAPMT) with 64 channels. The compact front-end electronics called

[1] **ALFA** stands for **A**bsolute **L**uminosity **F**or **A**TLAS

PMF [2], are directly mounted on the back of the MAPMT. The MAROC2 ASIC [2] allows to correct the MAPMT gain non-uniformity and to discriminate the signal. An FPGA ensures the communication with the motherboard fixed on the pot. On top of that, the *overlap detectors* sketched in Fig. 6 are used to measure the relative position between the upper and the lower pot with a precision of 10 μm. Mechanically fixed to the main tracker, they provide essential information about the t-scale that cannot be extracted from the data. This measurement will be done reconstructing the halo particles passing at the same time through the upper and lower overlap detector.

5 The Simulation

The acceptance of the ALFA detector is a major issue and has to be computed by simulation. Indeed, one has to know as precisely as possible which protons will pass through the sensitive area of the detectors and which will go in between the upper and lower pot or will be lost during the transport from the IP to the RPs. This simulation therefore includes:

- a Monte-Carlo generator (Pythia [3]) to generate the event according to the differential elastic cross section,
- transport software (MadX [4]) to track the protons along the magnetic lattice (see Fig. 7),
- reconstruction software to build the spectrum, correct it and fit it.

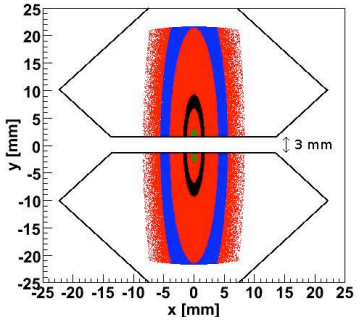

Figure 7: Scattering picture at the RP. The black lines show the diamond shape of the active part of the detector.

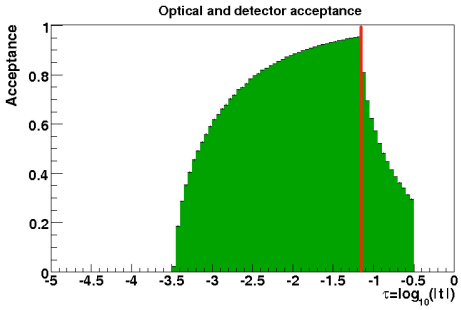

Figure 8: Acceptance obtained with the same parameters as define earlier.

Due to the optics settings, one t-value is seen as an ellipse in the detector. In Fig. 7 are sketched (x,y)-maps at the RP for three different t-ranges to give an idea of where the scattered protons will hit the detector. The inner ring represents $t \in \left[7\ 10^{-4}; 13\ 10^{-4}\ \text{GeV}^2\right]$, the middle one $t \in \left[7\ 10^{-3}; 13\ 10^{-3}\ \text{GeV}^2\right]$ and the outer one $t \in \left[7\ 10^{-2}; 13\ 10^{-2}\ \text{GeV}^2\right]$. The elastic protons detected allow to reconstruct the spectrum and to determine the acceptance. Fig. 8 shows the acceptance as a function of t for 7 TeV protons with the detectors at 12 σ from the beam center. One can observe two distinctive causes of acceptance losses. On the right of the red line, events are mainly lost in the accelerator due to the magnetic element aperture, and on

the left, protons are passing between the two pots. The acceptance determination will allow to correct the detected spectrum to recover the underlying physics distribution.

In Table 1 [1, 5] are summarized the contributions to the precision on the luminosity measurement from various sources. In the so-called beam properties part, the major impact will be from the angular divergence as it mainly affects small values of t for which the fit is very sensitive. However the measurement of the optical parameters will also be an important issue. The detector properties will be dominated by the detector alignment with respect to the beam and acceptance corrections. Any error on this measurement will drastically affect the result of the fit. The background is composed of beam-gas events, particles surviving the LHC collimation system and all non-elastic processes such as single diffraction events. Its rejection is done using mainly the back-to-back topology of the elastic event. The simulation has shown that the 2-3 % claimed in [1] on absolute accuracy can be reached.

	[%]
Beam properties	1.2
Detector properties	1.4
Backgroud substraction	1.1
Total uncertainty	2.1
Statistical error	1.8
Total	2.8

Table 1: Summary of the different uncertainties obtained on integrated luminosity for $\int L = 3.6\ 10^{32}\ \mathrm{cm}^{-2}$.

6 Detector Performances

The first complete tracker (20 planes of 64 fibers each) has been tested in August 2008 on the SPS test-beam line H8 at CERN. However, only half of the detector could be read out. The ALFA detector was coupled to a silicon strip telescope with a resolution of $10\,\mu$m. Using this setup we were able to determine the layer efficiency and the spatial resolution.

The layer efficiency has been computed using the telescope prediction. Indeed the accurate telescope resolution allows to point in each layer to the fiber where the particle went through. Comparing this prediction with the data allows us to determine the layer efficiency which has been found to be $\approx$90 %. Combining layers together this is enough to reach almost 100 % detection efficiency for the entire ALFA tracker.

The reconstruction method consist in projecting all fibers from all planes of the same orientation on a perpendicular plane. If a particle went through the detector, the hit fibers corresponding to the path will overlap on this projection. One can determine then the position of the center of the overlap region and its width. To accept a track in the reconstruction algorithm, a minimum of three fibers for half a detector must define the overlap region i.e. all layers do not have to be efficient, but only 60 % of them. For a full detector this limit is set to a minimum of 6 layers. This condition has a major impact on the resolution: the higher the number of fibers defining the track path is, the greater is the probability to have a small area of overlap providing a better resolution. This is exactly what we see in Fig. 9, which displays the resolution improving with a decreasing overlap region.

The spatial resolution obtained with half a detector is close to $52\,\mu$m in both directions. This results has been compared to a Monte Carlo simulation including layer efficiency and real geometry, and comparable results have been found. For a full detector, where the staggering configuration is optimal, the average overlap region width is lower than $100\,\mu$m. Judging by the Fig. 9 we can expect a resolution around $35\,\mu$m.

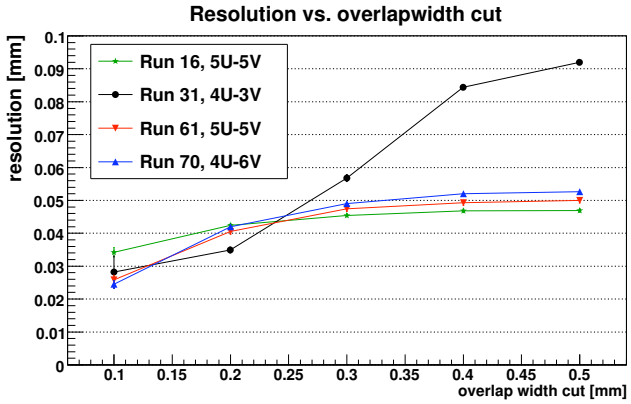

Figure 9: Resolution dependency on the overlap region width, #U and #V standing for the number of U-V layers used.

7 Conclusion

The studies of the systematics has shown that 2-3 % absolute accuracy on luminosity can be reached with the ALFA detector. All test-beam studies done so far have validated the technical choices made for the different parts of the ALFA detector. A new test-beam period is planned for October 2009 to definitely validate the electronics and the full tracker.

References

[1] CERN/LHCC/2008-004, ATLAS TDR 18, 17 January 2008.

[2] *PMF: the front end electronics of the ALFA detector*, Barrillon P., proceedings of 2008 IEEE conference.

[3] Pythia website, http://home.thep.lu.se/ torbjorn/Pythia.html

[4] MAD-X website, http://mad.web.cern.ch/mad/

[5] *Luminosity calibration from elastic scattering*, Stenzel H., CERN, Geneva ,ATL-LUM-PUB-2007-001